DOI: 10.4467/21995923GP.23.009.18608 GEOINFORMATICA POLONICA
22: 2023

Odunayo Tope Ojo[1]
ORCHID: 0000-0003-2973-6858

James Adejimi Adeoye[2]
ORCHID: 0000-0001-5441-299X

Okoli Emeka Austin[3]
ORCHID: 0000-0003-4777-1980

Joseph Onyeka Emegha[4]
ORCHID: 0000-0001-6392-8867

PETROPHYSICAL AND GEOMECHANICAL ANALYSIS TO DELINEATING RESERVOIRS IN THE MIOCENE NIGER DELTA REGION OF NIGERIA

[1] Department of Physical Sciences (Geology Program), Faculty of Natural Sciences, Redeemer's University, Ede, Osun State, Nigeria
[2] Department of Geology and Mining, Faculty of Applied Sciences and Technology,
Ibrahim Badamasi Babangida University, Lapai Niger State, Nigeria
[3] Department of Geology, School of Physical Science, Federal University of Technology, Owerri, Nigeria
[4] Department of Energy and Petroleum Studies, Novena University, Ogume, Delta State, Nigeria

Abstract

The application of various petrophysical and elastic metrics has advanced reservoir characterization and provided critical geological formation information. Porosity declines with depth, according to sonic, neutron, and density logs. Lithology, pressure, and hydrocarbons all contribute to this. Formation resistivity and fluid saturation are used to identify hydrocarbon-bearing zones. Because oil and gas are non-conductive, hydrocarbon-containing rocks are more resistant than water. In lithological categorization, gamma logs and the V_p/V_s ratio have helped classify reservoirs as Agbada Formation sand-shale reservoirs. Reservoir elastic characteristics, specifically sandstones, have been studied at various depths. These discoveries have an impact on their brittleness, strength, and failure risk in a variety of scenarios. Hydrocarbon accumulation has been influenced by diagenetic compaction equilibrium in pressure-exposed shale source beds. The research advances our understanding of the geological formations of the Niger Delta and gives practical insights for exploration and production. Decisions on oil and gas are based on hydrocarbon reservoir assessments at various depths, including porosity, fluid saturation, and lithology. Well logs from Wells B001, B002, and B003 revealed the diverse properties of several Niger Delta reservoirs. These discoveries have benefited hydrocarbon exploration and production decision-making significantly.

Keywords: reservoir characterization, hydrocarbon prospects, lithological classification, porosity trends, elastic properties

PETROFIZYCZNA I GEOMECHANICZNA ANALIZA W POMIARACH PROWADZONYCH NA ZŁOŻACH W OSADACH MIOCEŃSKICH W REJONIE DELTY NIGRU W NIGERII

Abstrakt

Charakterystykę zbiorników wodnych poszerzono dzięki różnym pomiarom petrofizycznym i pomiarom elastyczności, dostarczając wartościowych informacji o formacjach geologicznych. Określenia porowatości przy użyciu zapisów dźwięku, badania neutronów oraz gęstości wykazały wyraźną tendencję do zmniejszania się porowatości wraz z głębokością. Przyczynia się do

tego litologia, ciśnienie i obecność węglowodorów. Strefy węglowodoronośne są identyfikowane przez korelację pomiędzy tworzeniem się oporności a nasyceniem skał węglowodorami. Wyższa oporność skał nasyconych węglowodorami wynika ze złego przewodnictwa ropy naftowej i gazu, w porównaniu z wodą. Klasyfikacja litologiczna na podstawie zapisu gamma i ilorazu Vp/Vs doprowadziła do głębszego zrozumienia składu złóż, klasyfikując je jako złoża piaskowo-łupkowe formacji Agbada. Elastyczne właściwości złóż, szczególnie piaskowców, wykazały ważne korelacje związane z głębokością, która ma wpływ na kruchość złóż, ich odporność oraz podatność na zniszczenie w różnych warunkach. Obserwowana w złożach łupkowych pod ciśnieniem równowaga ścisłości diagenetycznej odegrała znaczącą rolę w akumulacji węglowodorów. Wyniki badań nie tylko przyczyniają się do zrozumienia formacji geologicznych w rejonie delty rzeki Niger, ale również dostarczają podstaw do przedsięwzięć związanych z poszukiwaniem i eksploatacją złóż. Charakterystyka złóż węglowodorowych na różnych głębokościach i ich cechy, takie jak porowatość, nasycenie płynem i litologia, przyczynią się do podejmowania decyzji w przemyśle naftowo-gazowym. Analiza danych z odwiertów B001, B002 oraz B003 pozwoliła na znalezienie cech charakterystycznych dla wielu złóż w rejonie delty Nigru, dostarczając wartościowych informacji dla podejmowania decyzji dotyczących poszukiwań i wydobycia węglowodorów.

Słowa kluczowe: charakterystyka złoża, prognozowanie ilości węglowodorów, klasyfikacja litologiczna, trendy dot. porowatości, właściwości elastyczne

1. INTRODUCTION

Identifying sandstone beds requires a thorough understanding of reservoir petrophysical properties, where cap rocks act as seals. This article examines the petrophysical and geomechanical properties of five Niger Delta offshore wells. Petrophysical criteria include apparent water saturation, limitless water saturation, porosity, bulk water volume, shale volume, and hydrocarbon saturation [1]. Geomechanical properties such velocity ratios, compressional and shear velocities, Poisson's ratio, bulk modulus, shear modulus, compressional impedance, and shear impedance are assessed. Gamma, Density, Neutron, Sonic, and Resistivity logs determine these attributes.

The terms „stone beds" and „cap rocks" are used interchangeably. A cap rock acts as an impermeable seal that encircles and lies above a hydrocarbon reservoir, effectively trapping hydrocarbon fluids beneath it. The recognition of cap rocks holds significance when searching for hydrocarbon reservoirs [2, 3]. Logging involves recording information concerning depth or time. Well-logging, especially in borehole geophysics, has diverse applications and significance [4]. It entails the study of various formations encountered within a well. In the context of oil exploration, the primary focus is on categorizing porous and permeable formations, understanding their dimensions and extent, and characterizing reservoir geometry [5].

The practical application of compressional wave velocity determined from past sonic logs or seismic velocity check shots is common in many existing oil fields. Shear wave velocities and moduli, on the other hand, are critical for applications such as amplitude variation with offset (AVO) inquiry, seismic modelling, and engineering goals. It is critical in these applications to obtain shear wave velocities or moduli from compressional velocities or moduli that are already available, either empirically or theoretically. According to [6], there is a linear relationship between P-wave velocity (Vp) and S-wave velocity (Vs) in saturated sandstones. Castagna (1985) [7] describes a method for determining shear velocity in shaly sandstones by taking porosity and clay concentration into account. There is a connection between V_p/V_s values and lithology, according to multiple log investigations undertaken by [8, 9, 10, 11]. This examination, in addition to assisting with lithology identification, provides vital information about the elastic behaviour of the material.

Using elastic constants to measure formation strength determines if it can tolerate high flow rates without sand generation. Inherent rock strength and elastic constants are connected. The sonic or acoustic log measures elastic wave velocity in a configuration by measuring their travel time.

Compressional wave velocity and rock elastic characteristics are connected by matrix and fluid components. Thus, wave deceleration depends on matrix constitution, microstructural characteristics, pore fluid dispersion, and rock porosity. P-wave velocity is directly proportional to material strength and inversely proportional to density. The decrease in P-wave velocity within a substance is proportional to its mechanical resistance and mass per unit volume.

Various geological processes, such as burial depth, lithology, anisotropy, and diastrophism, influence the elastic properties of rocks. Geological characteristics, in conjunction with porosity, determine the transit times of interest. The elastic properties of rocks are controlled more by their structure and geological history than by their mineral composition. According to [12], it is frequently found that crystalline rocks have higher elastic modulus values than fragmental rocks.

Hooke's law, a key principle in the study of elastic materials, states that the strain shown by such materials is proportionate to the applied stress as long as the stress remains within the elastic range. The term "stress" refers to the external force applied to a material divided by its area, and „strain" refers to the fractional deformation caused by the applied force. Depending on how the force is delivered, three types of deformation can occur. The modulus of elasticity is a measurement that measures the stress-strain relationship.

Agbasi et al., (2023) [13] states that reservoir factors including porosity, permeability, water saturation, thickness, and reservoir area extent affect producible hydrocarbon measurement. These metrics are important for reservoir studies because they accurately estimate hydrocarbon volume. Sandstone and unconsolidated sands in the Niger Delta, especially the Agbada formation, are used to extract petroleum. Since hydrocarbon reservoirs are the main extraction sites, their correct description and appraisal are crucial.

The systematic use of all available data to determine reservoir elements is reservoir characterisation. This method builds accurate reservoir models for accurate reservoir performance forecasting [14]. It is necessary to understand the water saturation levels in order to determine the hydrocarbon reserves contained in a geological formation [15]. The Nigerian Delta formations are distinguished by the abundance of sands and shales. Fluvial channels and fluvio-marine barrier bars are among the depositional habitats found in the sands. The shales, on the other hand, are often generated from fluvio-marine or lagoon settings. Because of the unconsolidated nature of these formations, core samples and drill stem testing are frequently impractical [16]. As a result, as illustrated in this study, assessing formation characteristics is heavily reliant on the use of well logs, supplemented by data from mud loggers and geological information. The study of well log data yielded petrophysical properties such as lithology, porosity, fluid content, hydrocarbon saturation, water saturation, and permeability. The primary goal of this research is to investigate the petrophysical properties and geomechanical characteristics of reservoirs in an oil and gas field in the Niger Delta region. This goal will be met by reviewing well log data.

2. LOCATION OF THE STUDY AREA

The Niger Delta is a huge hydrocarbon province of global importance located on the Gulf of Guinea in the western part of central Africa, namely in Southern Nigeria. The study area extends from longitudes 4°E to 9°E and latitudes 4°N to 9°N. It is distinguished by a dominating regressive clastic succession with a maximum thickness of approximately 12 km [17].

The Niger Delta region is divided into three geological formations, according to [18]: the Benin Formation, which represents the continental top facies, the Agbada Formation, and the AkataFormation. The Benin Formation is the geological sequence's shallowest stage, composed mostly of continental sands and gravels containing freshwater. The fluviomarine-derived sand and shale dominate the Agbada Formation, which lies beneath the Benin Formation. This geological deposit is important since it is the primary hydrocarbon reservoir [19]. The Akata Formation, located toward the bottom of the known delta series, is primarily composed of shale, clay, and silt deposits. Sand bands may have evolved as a result of turbiditic processes in the landscape. Although the precise thickness of this series is uncertain, it is expected to reach up to 7000 meters in the delta's center part [18]. The research focuses on the offshore depobelt in the Niger Delta.

The Niger Delta Depobelt consists of five distinct stratigraphic sections: Northern Delta, Ughelli, Central Swamp, Coastal Swamp, and Offshore Delta. The Northern Delta province has the oldest growth faults, which are situated atop a shallow basement [19]. These faults exhibit rotational displacement, consistent intervals, and a progressively sharper inclination towards the ocean. In the Central Delta province, depobelts exhibit distinct formations, such as consecutive rollover crests that gradually move towards the sea along each growing fault.

The Niger delta region has been considered the most structurally intricate due to internal gravity-driven tectonic processes occurring on the contemporary continental slope. Petroleum extraction in the Niger Delta

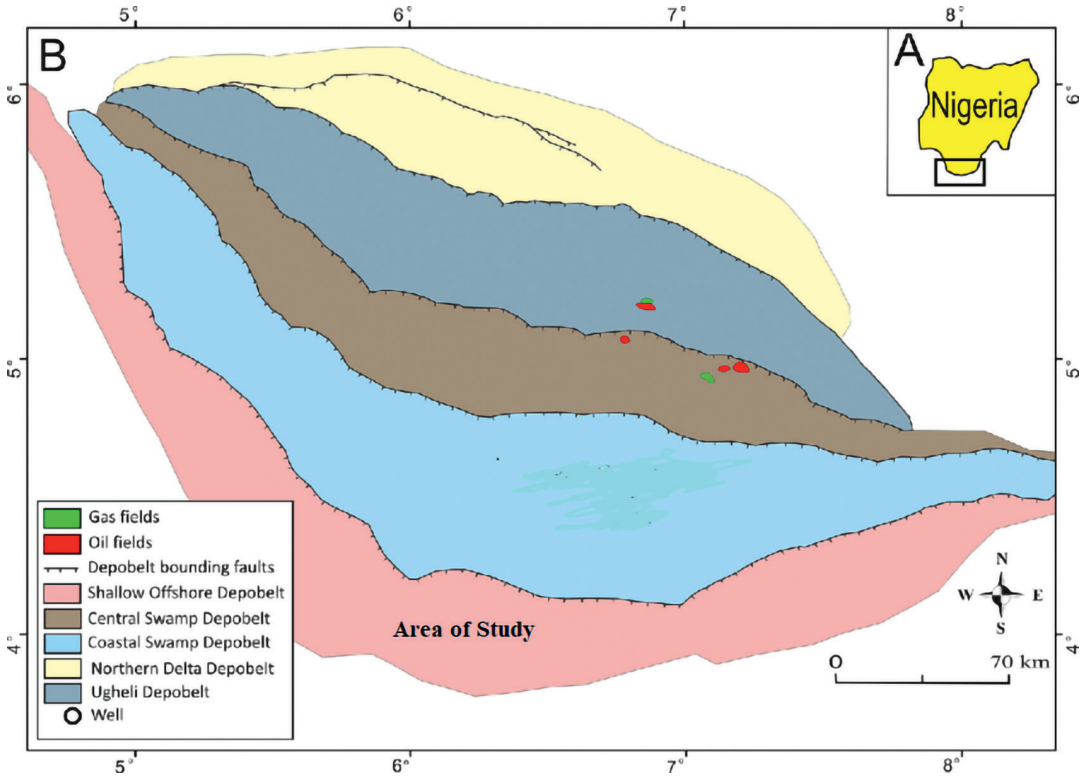

Fig. 1. Niger Delta Depobelt showing Study Area
Ryc. 1. Obszary akumulacji w delcie rzeki Niger, widoczny obszar badań

region primarily focuses on the exploitation of sandstone and loosely cemented sands found within the Agbada Formation. The reservoir features observed in this formation are subject to the influence of both the depositional environment and the depth of burial. The reservoir rocks, which span from the Eocene to Pliocene epochs, frequently exhibit a stacking arrangement. The thickness of these geological formations exhibits variation, with approximately 10% of them surpassing a thickness of 45 meters [20].

Stratigraphic traps also exist in the Niger Delta region, with the structural complexity increasing from the depobelts in the north to the southern region. The sandstone-shale series undergoes a slow shift towards the delta toe, resulting in a predominance of sandstone. The predominant sealing lithology in the Niger Delta region is the intercalated shale layers found within the Agbada Formation [18]. The shale functions as a seal by three distinct mechanisms: the presence of clay smears along faults, the juxtaposition of interbedded sealing units against reservoir sands as a result of faulting, and the formation of vertical seals.

Materials and Methods

Geological data were gathered from five fields within the Niger Delta depobelt. The primary logs employed for distinguishing lithology included gamma ray, resistivity, sonic, compensated neutron porosity, and density logs. The analysis procedure comprised two main segments: petrophysical analyses and geomechanicalanalyses. Within the petrophysical realm, the process involved conditioning and refining the logs to establish the lithology log (gamma), incorporating density, neutron, and sonic logs, as well as formation factor (resistivity), water saturation, saturation, lithology, and areas of particular interest.

The outcome of log analyses, in terms of reservoir parameters, is provided by well logging interpretation. This interpretation is instrumental in deriving values for porosity, water saturation, and hydrocarbon saturation through the application of Archie's equation [21]. Quick look log interpretation is frequently used for pinpointing hydrocarbon zones via well logs. Several parameters aid in identifying reservoir zones, often dis-

cerned by gamma ray and resistivity logs. The resistivity log plays a pivotal role in differentiating shaly sand beds, given that hydrocarbons are non-conductive. Thus, gamma ray logs assist in recognizing clean sand and sandstones by detecting the presence of radioactive isotopes like thorium, uranium, and potassium, which tend to be more concentrated in shale and less so in sandstones. The resistivity curve can also offer insights into the presence of hydrocarbons within porous and permeable rocks.

3. PETROPHYSICAL ANALYSIS

Porosity refers to the proportion of voids relative to the total rock volume. The assessment of porosity holds significant importance for petroleum engineers, as it dictates the reservoir's ability to store oil and gas. Typically, water saturation tends to rise with depth, while porosity diminishes due to compaction [22].

This property is often expressed as either a decimal fraction or a percentage, conventionally denoted by the Greek letter phi (ϕ).

$$\phi = \frac{Volume\,of\ pores}{Total\,volume\ of\ rock} \tag{1}$$

The amount of internal space or voids in a given volume of rock is a measure of the amount of fluid rock will hold. The porosity logs include sonic log, density log and neutron log.

The sonic log functions as a porosity log, assessing the interval transit time (Δt) of compressional sound waves as they traverse a foot of formation. Expressed in microseconds per foot, the interval transit time (Δt) serves as the inverse of the velocity of a compressional sound wave, measured in feet per second. This parameter is influenced by both lithology and porosity [23].

The porosity calculated from the sonic log is chosen to ascertain porosity under favourable borehole conditions and is derived from the following equation:

$$\phi sonic = \frac{\Delta tlog - \Delta tma}{\Delta tf - \Delta tma} \tag{2}$$

Equation (2) is known as Wyllie Time Average Porosity, $\phi sonic$ = sonic derived porosity, Δtma = interval transit time of the matrix, Δtlog = interval transit time of formation is the reading on the sonic log in us/ft, Δtf = interval transit time of the fluid in the bore (fresh water = 189, salt = 185).

Where a sonic log is used to determine porosity in unconsolidated sands, an empirical factor (Cp) is applied to equation (2)

$$\phi sonic = \left(\frac{\Delta tlog - \Delta tma}{\Delta tf - \Delta tma}\right) \times 1/Cp \tag{3}$$

Cp (compaction factor) is obtained from the formula

$$Cp = \frac{\Delta tsh \times C}{100} \tag{4}$$

t_{sh} = interval transit time for adjacent shale,
C = a constant which is normally 1.0.

The formation density log, functioning as a porosity log, quantifies the electron density of the formation. This log aids in the identification of evaporate minerals, the detection of gas-bearing zones, the determination of hydrocarbon density, and the evaluation of shaly sand reservoirs and lithology [23].

The density log serves a dual purpose, facilitating lithology discrimination and enabling the calculation of porosity and hydrocarbon density. The measurement scale typically ranges from 1.95 to 2.95, expressed in g/cm³ [24].

Porosity derived from density is computed using the following equation:

$$\phi d = \frac{^{\delta}ma - {}^{\delta}b}{^{\delta}ma - {}^{\delta}f} \tag{5}$$

$^{\delta}$ma is density of rock matrix, $^{\delta}$b is bulk density of formation fluid, $^{\delta}$f is the density of formation fluid.

The matrix Densities of common lithologies used in the density porosity formula as adopted by Schlumberger is as follows:

Table 1. Matrix of common lithologies (After Schlumberger, 1987) [25]
Tabela 1. Skała macierzysta wspólnej litologii (wg Schlumberger, 1987) [25]

Lithologies	(g/cc)
Sandstone	2.648
Limestone	2.71
Dolomite	2.876
Anhydrite	2.977
Salt	2.032

These logs are used to measure the concentration of hydrocarbon ions in a formation, indicating porosity. When pores are filled with gas instead of oil or water, neutron porosity values decrease [23]. Neutron and density logs are sometimes combined to create a Neutron-Density log, which helps determine lithology and identify gas-bearing zones. Porosity in a gas zone can be calculated using the following formula:

$$\phi NDgas = \sqrt[1]{\frac{\phi^2 N + \phi^2 D}{2}} \tag{6}$$

$^{\delta}$ N is neutron porosity,
$^{\delta}$D is the density porosity.

The criterion for classifying porosity is given:

Ø < 0.05 = Negligible, 0.05 < Ø < 0.1 = Poor,
0.1Ø < 0.15 = Fair, 0.15 < Ø < 0.25 = Good,
0.25 < Ø < 0.30 = Very good, Ø > 0.30 = Excellent.

Resistivity logs are electrical measurements that assess a formation's resistance to the flow of an electric current. Because the rock matrix or grains are non-conductive, the current's conduction primarily depends on the presence of water within the pores. Hydrocarbons, akin to the rock matrix, are non-conductive. Consequently, as the saturation of hydrocarbons in the pores rises, the rock's resistivity also increases [26].

Lithology classification is performed by utilizing gamma ray and density logs. By analysing the gamma ray log, it becomes possible to identify sequences of sandstones, shales, and carbonates [27]. The provided table outlines the gamma ray reading ranges associated with various lithologies. Additionally, to differentiate between sandstone and carbonate, the density log is employed in conjunction with the gamma ray log.

Table 2. Gamma ray reading for different lithologies [27]
Tabela 2. Odczyt promieniowania gamma dla różnych litologii [27]

Lithology	Range (API)
Carbonates	< 15
Sandstones	>15 and < 40
Shaly Sandstones	>40 and < 65
Sandy Shale	>65 and < 80

The main step before calculating the shale volume is to calculate the gamma ray index, which can be calculated by the following [24]:

$$I_{GR} = \frac{GRlog - GRmin}{GRmax - GRmin} \tag{7}$$

Where:
I_{gr} = Index of Gamma ray,
GR_{log} = Gamma ray Log,
GR_{max} = Gamma ray maximum,
GR_{min} = Gamma ray minimum.

The gamma ray (GR) log stands as the most commonly employed technique for quantifying shale volume. When quantitatively assessing shale content, the underlying assumption is that non-radioactive minerals are present in clean rocks.

$$V_{sh} = \frac{GRlog - GRmin}{GRmax - GRmin} \tag{8}$$

Water saturation can be obtained from formation factor as follows

$$\mathrm{F} = \frac{Ro}{Rw} \tag{9}$$

R_o is the resistivity of formation, R_w is the resistivity of saturating water

If hydrocarbon is present, the resistivity of formation is Rt and water saturation is less than 100%. But

$$\mathrm{F} = \frac{Ro}{Rw} = \frac{a}{\phi^m} \tag{10}$$

Where α is the texture of the rock, ϕ is the porosity, m is the cementation factor, α varies from 0.6 to 2.0, depending on texture,m varies from 1–3 according to the type of sediment.

Water saturation can be deduced from Archie equation as

$$\mathrm{Sw}^n = \frac{Ro}{Rt} \tag{11}$$

From (11):

$$R_0 = \frac{aRW}{\mathrm{Rt}\ \phi^m} \tag{12}$$

From (11) and (12) we have

$$S_w = \sqrt[n]{\frac{aRw}{\mathrm{Rt}\ \phi^m}} \tag{13}$$

Where n is saturation exponent and lies between 1.2 to 2.2 or 1.5 to 3 or 2 [29].

From water saturation S_w, hydrocarbon saturation can be calculated using the formula

$$S_h + S_w = 1 \tag{14}$$

The bulk volume of water (BVW) is calculated as the product of the formation's water saturation and its porosity.

$$BVW = S_w \times \phi \tag{15}$$

4. GEOMECHANICAL ANALYSIS

Several geomechanical parameters, such as Poisson's ratio, bulk modulus, Young's modulus, shear modulus, compressibility, unconfined compressive strength (UCS), porosity, and shale volume, are calculated using well-log data. In this scenario, we will calculate the bulk modulus, shear modulus, Young's modulus, and Poisson's ratio using the gathered well logs. The data was entered into software for analysis, with a focus on using rock physics to interpret shear sonic readings.

To accomplish this goal, the Greenberg Castagna Model was used. The study's input parameters were compressional sonic, DTs Emp, and density. These parameters were used to determine Vp, Vs, Poisson's Ratio, Vp/Vs Ratio, Bulk Modulus (KB), and Shear Modulus (Mu). The impedances were estimated using the formula 304.8 * (Density / DTsEmp), with Alc curves selected and the program executed after the transition to Als curves [30].

The obtained output data was imported into an Excel spreadsheet and then formatted in Microsoft Office Word to generate a comprehensive tabulated presentation. Hooke's law, a key principle in the study of elastic materials, asserts that the resulting deformation is directly proportional to the applied force under elastic conditions. The term stress refers to the external force exerted on a material per unit area, whereas strain reflects the proportionate deformation caused by the applied force. The classification of deformation types is determined by the specific manner in which the externally applied force is exerted. The modulus of elasticity is a measure of the stress-strain relationship.

The elastic moduli encompass:

Young's Modulus,

$$Y = \frac{\left(F/A\right)}{\left(dl/l\right)} \tag{16}$$

Bulk Modulus, B: this is the extent to which a material can withstand isotropic squeezing.

$$B = \frac{\left(F/A\right)}{\left(dv/v\right)} \tag{17}$$

Shear Modulus, S: this is the extent to which a material can withstand shearing.

$$S = \frac{\left(F/A\right)}{\tan s} \tag{18}$$

In the given context, F/A represents the force per unit area, dl/l denotes the fractional strain of length, dv/v represents the fractional strain of volume, and tan s represents the fractional strain of shape.

Poisson's Ratio, an additional significant elastic constant, is defined as the quotient of the strain occurring in a direction perpendicular to the strain in the direction of the applied extensional force.

Poisson's Ratio,

$$P = \frac{\left(dx/x\right)}{\left(dy/y\right)} \tag{19}$$

Let x and y represent the starting dimensions, and dx and dy represent the changes in the x and y directions as a result of the application of deforming stress in the y direction.

As one moves from the solid to the liquid to the gas phase, the intermolecular distances increase. As a result of this phenomena, solids have much lower compressibility than liquids and gases. The bulk modulus is the inverse of compressibility and is sometimes referred to as the coefficient of incompressibility [12].

The development of a relationship between sonic wave velocities and elastic constants is an important issue in the field of well logging parameters, especially when practical units are considered. The four elastic constants are expressed as:

Shear Modulus $G = \dfrac{a\rho_b}{\Delta T_s V}$ (20)

Bulk Modulus $\mathrm{K}_b = \rho_b \left(\dfrac{1}{\Delta T_c^2} - \dfrac{4}{3\Delta T_s^2} \right)$ (21)

Young's modulus $\mathrm{E} = 2\mathrm{G}\left(1 + v\right)$ (22)

Poison's Ratio $v = 0.5 \left(\dfrac{V_p}{V_s} \right) - \dfrac{1}{\left(\dfrac{V_p}{V_s} \right)^2} - 1$ (23)

The shear modulus holds significant importance as an elastic metric for evaluating and comparing the strength characteristics of various formations. The concept of a unified strength modulus has been established.

$$K = K_b + \frac{4}{3}G \tag{24}$$

which is same as

$$k = a\rho_b\left(\frac{1}{\Delta T_c^2} - \frac{4}{3\Delta T_s^2}\right) + \frac{4}{3}\frac{a\rho_b}{\Delta T_s v} \tag{25}$$

This composite modulus aligns well with recognized formation strength conditions. Prior to computing the composite modulus values, adjustments to the log data are necessary to account for hydrocarbon influences.

5. RESULTS AND INTERPRETATION

5.1. Petrophysics

Figure 2 displays the comprehensive well log for Well B001, highlighting the three focal reservoirs. Reservoir 1 spans from depths of 11310ft to 11336ft, Reservoir 2 covers depths between 11613ft and 11646ft, while Reservoir 3 occupies the depth range of 12405ft to 12407ft.

Figure 3 illustrates the depiction of Reservoir 1. The depth span of this zone lies between 11310ft and 11336ft. This selection is predicated on the attribute's characteristic to a favourable hydrocarbon reservoir: exhibiting low gamma ray readings, high resistivity, demonstrating neutron density crossover, and encompassing a substantial expanse of porous sand. A comprehensive analysis of these characteristics can be found in Table 3.

The upper and lower boundaries of the reservoir span from depths of 11310ft to 11336.5ft, with a net interval of 27.0 ft. Density exhibits a range from a minimum of 2.032 g/cm³ to a maximum of 2.309 g/cm³, with an average of 2.14 g/cm³. The gamma ray measurement registers 32.41 GAPI as its minimum, 108.057 GAPI as its maximum, and a mean value of 59.684 GAPI.Neutron values range between 0.255 v/v (minimum) and 0.375 v/v (maximum), with an average of 0.322 v/v. The resistivity readings within this reservoir vary from 2.023 Ωm (minimum) to 84.45 Ωm (maximum), with a mean value of 43.669 Ωm. Bulk water volume spans

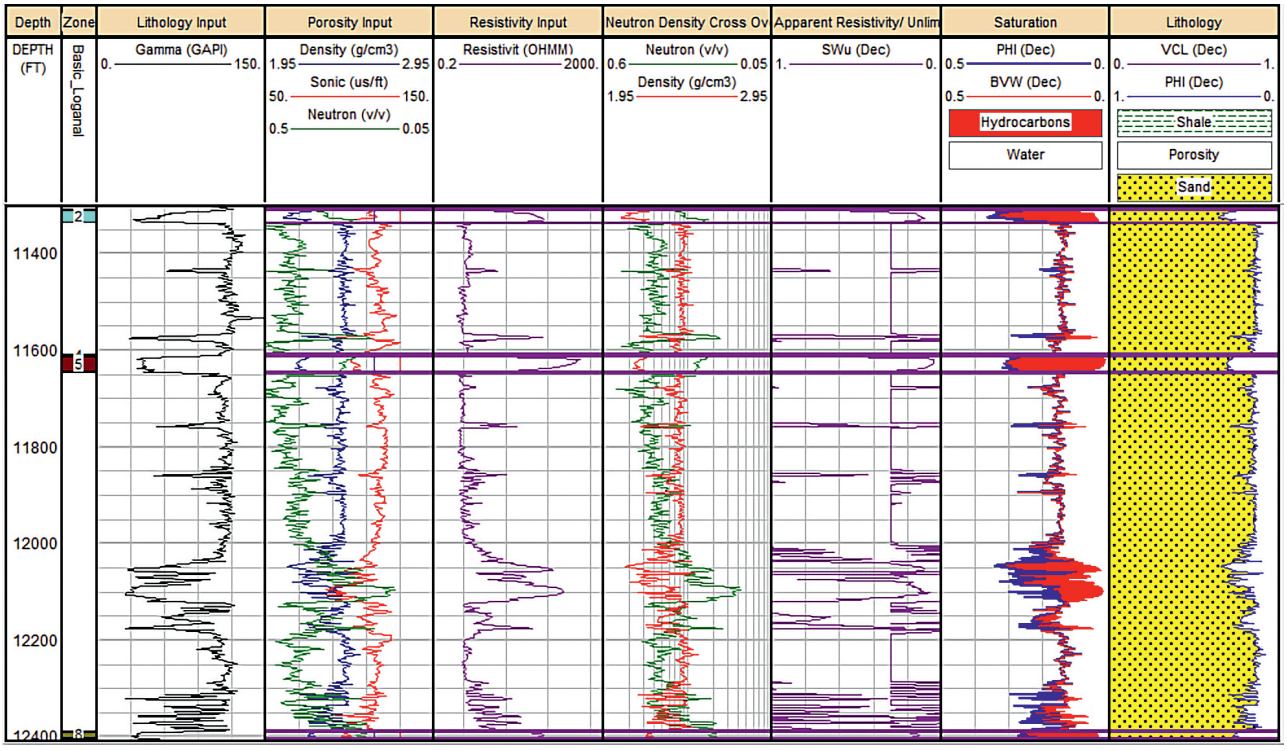

Fig. 2. Showing Complete Well log of well B001
Ryc. 2. Kompletny zapis odwiertu B001

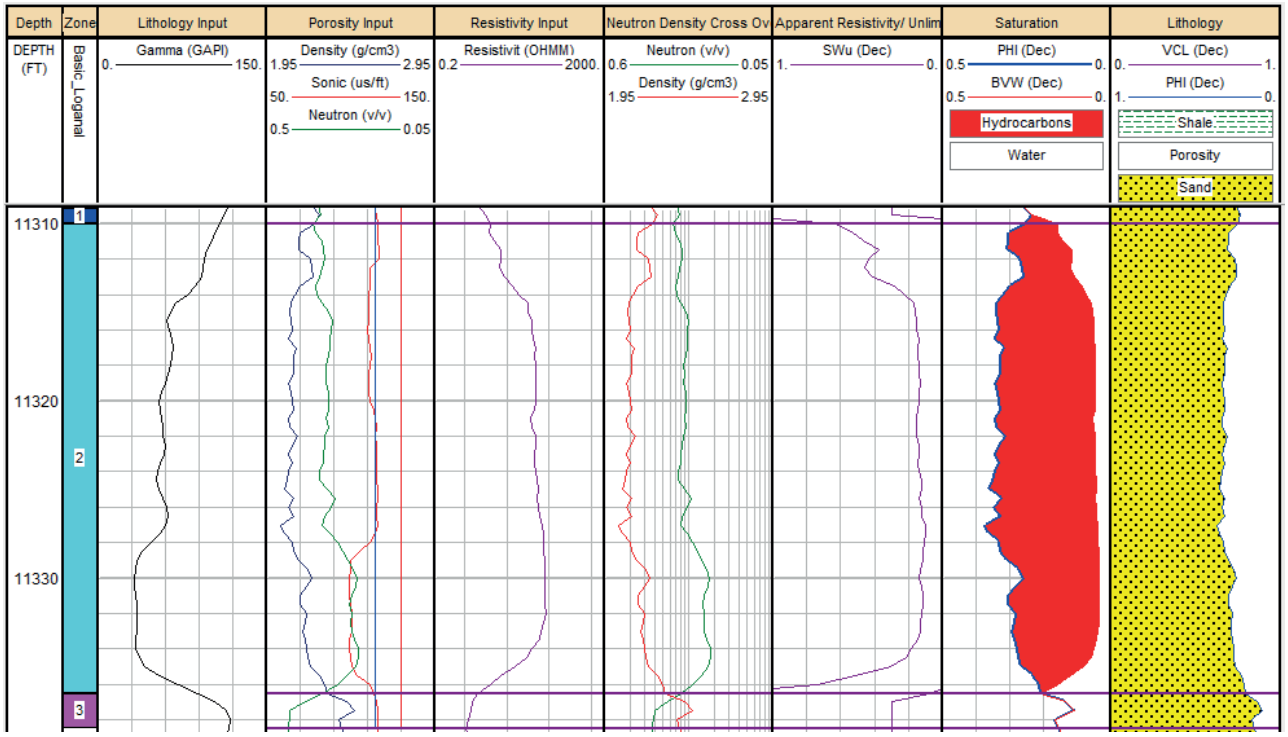

Fig. 3. Showing Reservoir 1, Top and Bottom Cap Rocks of Well B001
Ryc. 3. Rezerwuar 1, dolne i górne warstwy odwiertu B001

Table 3. Showing Input logs and Estimated Petrophysical Analysis of Reservoir 1 Well B001
Tabela 3. Zapisy wejściowe i oszacowane analizy właściwości fizycznych skał rezerwuaru 1 odwiertu B001

anCurve	Units	Top: 11310.000ft, Bottom: 11336.500ft, Net: 27.000ft		
		Min	Max	Mean
Density	g/cm^3	2.032	2.309	2.14
Neutron	v/v	0.255	0.375	0.322
Gamma	GAPI	32.41	108.057	59.684
Sonic	us/ft	98.961	116.861	109.88
Resistivity	Ohmm	2.023	84.45	43.669
BVW	Dec	0.034	0.207	0.064
SW	Dec	0.102	1	0.222
PHI	Dec	0.207	0.375	0.309
Vsh	Dec	0	0	0
SWu	Dec	0.102	1.075	0.223
RWapp	Ohmm	0.087	9.519	4.427

from 0.034 Dec (minimum) to 0.207 Dec (maximum), and the mean bulk water volume is 0.064 Dec.

Sonic measurements encompass a range of 98.961 us/ft (minimum) to 116.861 us/ft (maximum), with an average sonic value of 109.85 us/ft. Porosity values have an average of 0.309, varying from a minimum of 0.207 to a maximum of 0.375. Water saturation ranges from 0.102 (minimum) to 1.075 (maximum), and the

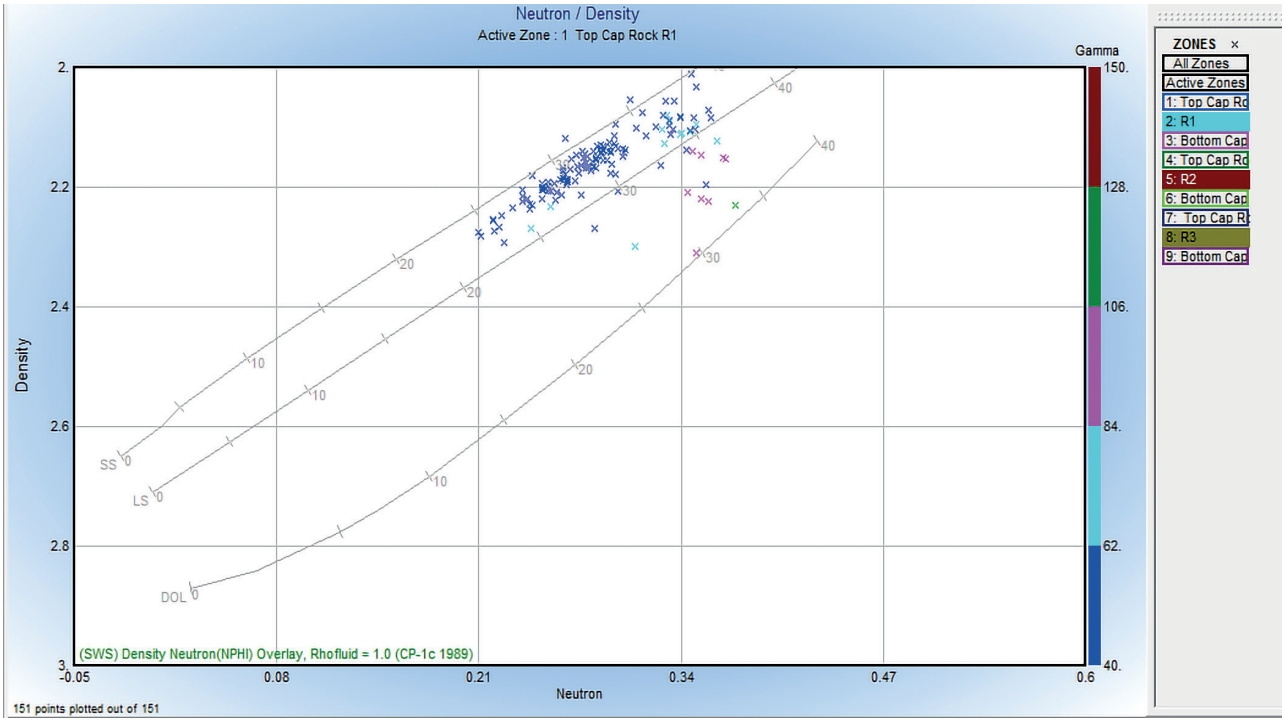

Fig. 4. Showing Neutron -Density Cross Plot of Well B001
Ryc. 4. Zestawienie neutron-gęstość w odwiercie B001

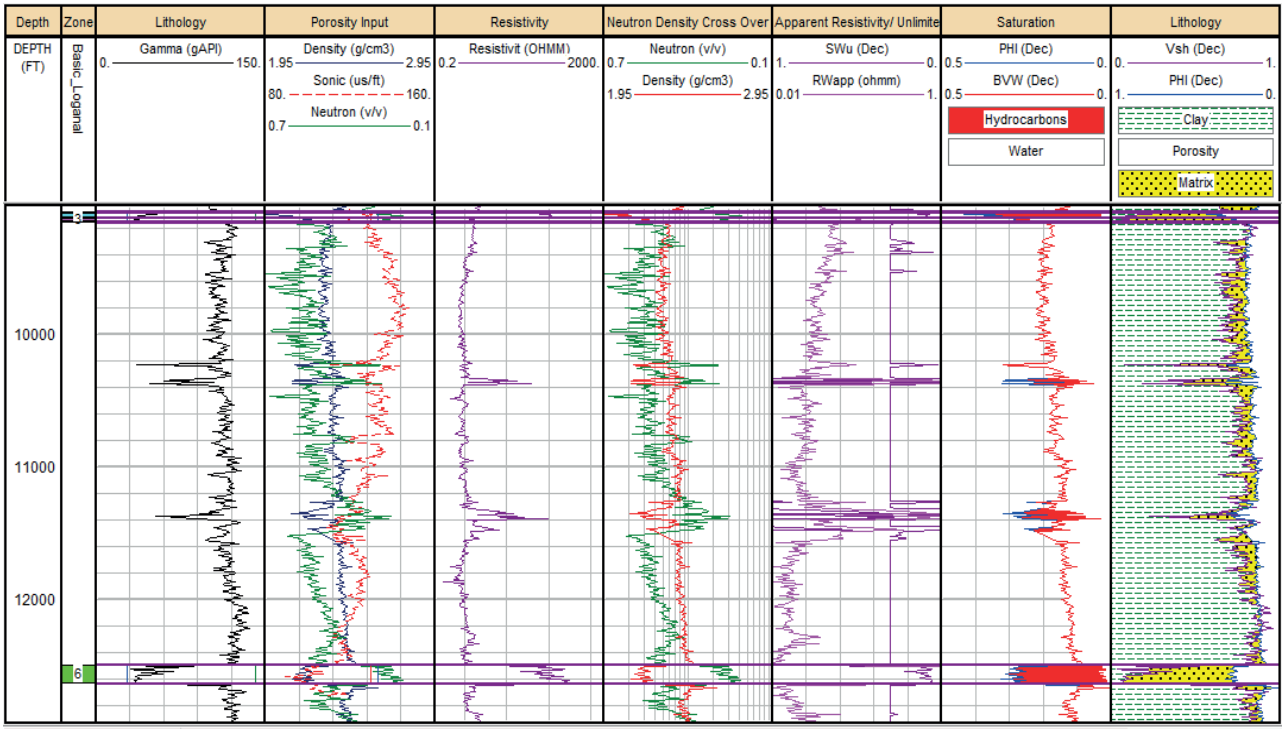

Fig. 5. Showing Complete well log of well B002
Ryc. 5. Całkowity zapis z odwiertu B002

mean water saturation is 0. 222.The apparent water resistivity of the well exhibits a range from 0.087 Ωm (minimum) to 9.519 Ωm (maximum), with an average of 4.227 Ωm. Notably, there is no shale present within the well.

Figure 4 displays the Neutron-Density Cross plot. This plot features density along the y-axis, neutron on the x-axis, and gamma on the extended y-axis.

The complete well log of Well B002 showing the two reservoirs with a water bearing zone is presented on Figure 5.

Reservoir 1, with its depth ranging from 9084.319ft to 9125.819ft. This selection is driven by the attributes associated with a favourable hydrocarbon reservoir: demonstrating low gamma ray readings, elevated resistivity, exhibiting neutron density crossover, and containing a substantial expanse of porous sand. The comprehensive analysis of these characteristics can be found in Table 4.

The density values exhibit a range from a minimum of 1.884 g/cm³ to a maximum of 2.363 g/cm³, with a mean of 2.089 g/cm³. Gamma ray measurements register a minimum value of 33.550 GAPI and a maximum of 04.56 GAPI, with an average of 46.554 GAPI. Neutron values range between 0.189 v/v and 0.398 v/v, with a mean of 0.263 v/v.Resistivity readings within this reservoir span from 2.260 Ωm to 1047.070 Ωm, with an average of 95.708 Ωm. Sonic measurements range from 116.856 us/ft to 144.440 us/ft, with a mean value of 127.218 us/ft. Bulk water volume values encompass a range from 0.010 Dec to 0.210 Dec, with a mean of 0.051 Dec.

The mean porosity value is 0.337, varying from a minimum of 0.163 to a maximum of 0.460. Water saturation ranges from 0.030 to 1.000, with an average water saturation of 0.191. The apparent water resistivity of the well varies from 0.085 Ωm to 108.474 Ωm, with a mean of 12.344 Ωm.Water saturation exhibits a range from 0.030 to 1.087, with an average of 0.192. Minimal shale content is recorded, with values of 0.057, 0.591 and 0.171.

5.2. Geomechanical Interpretation

The geomechanical well log for Well B001 provided a complete analysis of the three different reservoirs present within the well, which exhibited variable depths. Reservoir 1 had an increase in depth from 11310.000ft to 11336.000ft. Reservoir 2 exhibited a depth range spanning from 11613.000ft to 11646.000ft. Reservoir 3 contained depths ranging from 12405.000ft to 12407.000ft. In a similar vein, the cap rocks associated with these reservoirs displayed a wide range of depths.

The uppermost cap rock of Reservoir B001 exhibited a depth range extending from 11308.000ft to 11310.000ft, resulting in a net depth of 2.500ft. In con-

Table 4. Showing Input and Estimated logs for Petrophysical Analysis of Reservoir 1 Well B002
Table 4. Zapisy wejściowe i oszacowane analizy właściwości fizycznych skał złoża 1 odwiertuB002

Curve	Units	Top:9084.319ft, Bottom: 9125.819ft, Net: 42.000ft		
		Min	Max	Mean
Sonic	us/ft	116.856	144.44	127.218
Density	g/cm³	1.884	2.363	2.089
Gamma	GAPI	33.55	94.56	46.554
Neutron	v/v	0.189	0.398	0.263
Resistivity	Ohmm	2.26	1047.07	95.708
BVW	Dec	0.01	0.21	0.051
SW	Dec	0.03	1	0.191
SWu	Dec	0.03	1.087	0.192
PHI	Dec	0.163	0.46	0.337
Vsh	Dec	0.057	0.591	0.171
RWapp	Ohmm	0.085	108.474	12.344

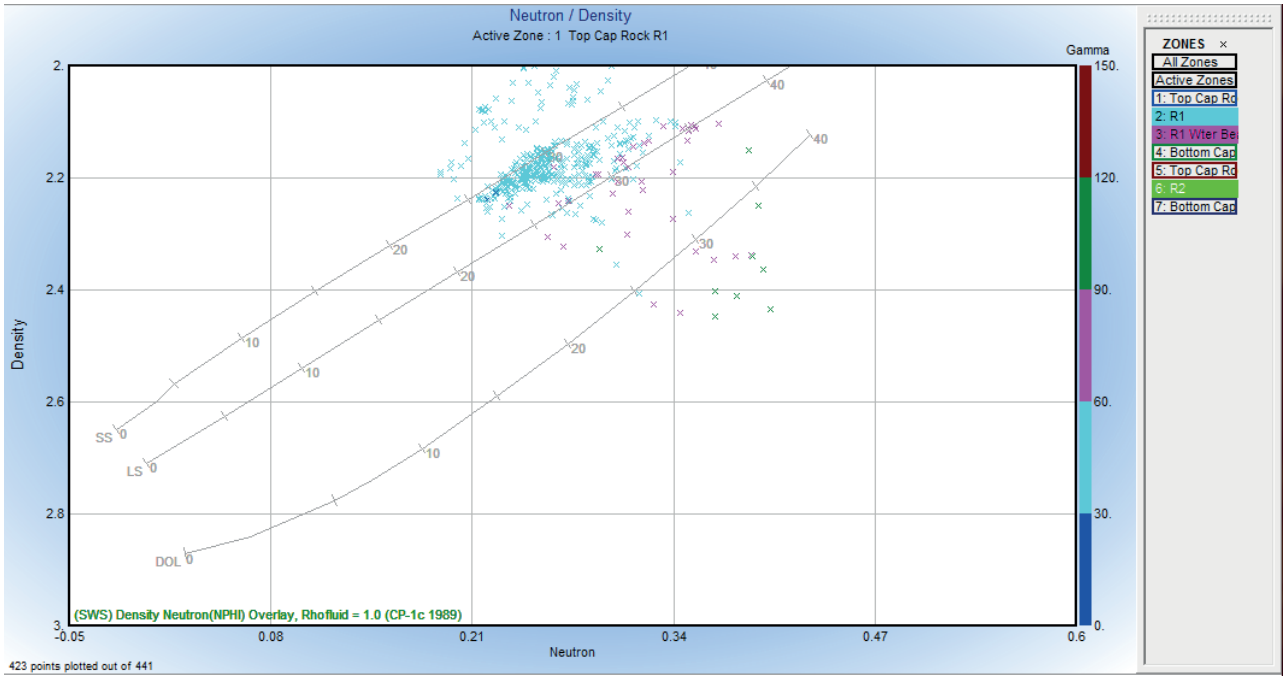

Fig. 6. Showing the Neutron-Density Cross Plot of Well B002
Ryc. 6. Zestawienie neutron-gęstość odwiertu B002

trast, the lower cap rock of the aforementioned reservoir exhibited a depth range of 11336.500ft to 11338.500ft, resulting in a net depth of 2.500ft. In relation to Reservoir B002, it is observed that the upper cap rock spans from a depth of 11608.500ft to 11613.000ft, covering a vertical distance of 5.000ft. In a similar vein, the lower cap rock of the reservoir exhibited depths ranging from 11645.000ft to 11647.500ft, resulting in a net depth of 3.000ft.

In the case of Reservoir B003, it was observed that the upper cap rock extended in depth from 12387.500ft to 12389.500ft, resulting in a net difference of 2.500ft. The cap rocks are of utmost importance in the containment of reservoirs and the preservation of the structural integrity of formations containing hydrocarbon deposits.

The geomechanical well log for Well B002 is a thorough representation of the two unique reservoirs present in the well. These reservoirs are located at various depths within the well. Reservoir 1 exhibited a vertical extent of from 9084.319ft to 9125.819ft, with a net depth of 42.000ft. The water-bearing zone inside this reservoir covered from 9125.819ft to 9157.819ft, with a net depth of 32.500ft. On the other hand, Reservoir 2 extended from 12492.319ft to 12637.819ft, with a net depth of 146.000ft. In addition, the cap rocks that are linked to these reservoirs had different depth intervals.

In relation to Reservoir 1 of Well B002, the depth of the upper cap rock varied between 9079.319ft and 9084.319ft, resulting in a net depth of 5.500ft. Conversely, the underlying cap rock of the aforementioned reservoir exhibited a vertical range extending from 9157.819ft to 9164.819ft, resulting in a total depth differential of 7.500ft. Moving on to Reservoir 2, the upper cap rock spanned from a depth of 12488.319ft to 12492.319ft, resulting in a total vertical extent of 4.500ft. In a comparable manner, the underlying cap rock of the reservoir exhibited depths ranging from 12637.819ft to 12639.819ft, resulting in a net depth of 2.500ft.

The cap rocks play a crucial role in delineating the boundaries of the reservoirs and enhancing their overall stability and containment.

The entire geomechanical well log for Well B003. This phenomenon effectively spans three separate reservoirs, each occupying discrete intervals of depth. The dimensions of the reservoirs are as follows: Reservoir 1 increased in length from 8784.250ft to 8804.000ft, resulting in a net depth of 20.000ft. Reservoir 2 stretched from 8851.750ft to 8902.000ft, with a net depth of 50.500ft. Lastly, Reservoir 3 spanned from 10270.750ft

to 10300.000ft, with a net depth of 29.500ft. Furthermore, the cap rocks that are linked to these reservoirs displayed different ranges in terms of depth.

Reservoir 1 of Well B003 exhibited an upper cap rock depth interval spanning from 8764.250ft to 8768.250ft, resulting in a net depth of 4.250ft. The bottom cap rock of the reservoir exhibited a vertical range extending from 8813.500ft to 8816.500ft, resulting in a net depth of 3.250ft. Moving to Reservoir 2, the upper cap rock spanned from a depth of 8849.000ft to 8850.500ft, covering a vertical distance of 1.750ft. In a similar vein, the bottom cap rock of the reservoir exhibited depths ranging from 8901.750ft to 8905.750ft, resulting in a net depth of 4.250ft. Finally, in the case of Reservoir 3, the upper cap rock exhibited a range of depths, spanning from 10266.750ft to 10269.000ft, resulting in a net vertical distance of 2.500ft. The lower cap rock of the reservoir exhibited a range of depths from 10300.750ft to 10302.500ft, resulting in a net depth of 2.000ft.

The cap rocks are of utmost importance in delineating the limits of the reservoirs and making substantial contributions to their stability and confinement.

6. DISCUSSION

The determination of porosity in reservoirs containing hydrocarbons was conducted by the use of acoustic, neutron, and density logs. The observed logs displayed a characteristic decline in porosity as depth increased. Within the Niger Delta region, a discernible pattern has been identified whereby the shale lithology exhibits a rising trend and the sandstone lithology demonstrates a declining trend as depth increases. This discovery is consistent with prior research conducted by [31,32,33], which suggests that as the depth of burial increases, porosity decreases. The aforementioned relationship highlights the fact that porosity is affected by both lithology and depth, wherein an increase in shale volume corresponds to a decrease in porosity.

The decline in porosity as depth increases might also be attributed to variations in pressure. Porous rocks, when exposed to pressure at certain depths, exhibit both reversible and permanent alterations in their porosity. The phenomenon of overburden pressure can exert an influence on the preservation of porosity at significant depths located above zones of overpressure. Moreover, [29] have emphasised that confining pressure plays a significant role in determining porosity within a specific depth and lithology. Porosity preservation can be influenced by the existence of hydrocarbons, as shown by [34]. It is imperative to acknowledge that, notwithstanding the intrusion of hydrocarbons, the reduction in porosity can still occur as a result of compaction.

A thorough examination was undertaken to analyse hydrocarbon intervals in five wells located inside the Niger Delta Fields. This investigation incorporated both petrophysical and elastic factors and applied a range of geophysical well logs [26]. The examination of geological logs, encompassing gamma-ray and electrical resistivity measurements, has unveiled a comprehensive spectrum of porosity values ranging from 15.0% to 84.0% within the hydrocarbon-rich stratum. In a similar manner, the water saturation exhibited a range of values, spanning from 11.1% to 60.0%. Significantly, a robust lithological link was identified among the fields that were examined. The study revealed that a significant proportion of hydrocarbons found in the Niger Delta basin were located at depths ranging from 3,500.5 to 11,507 feet (1,067 to 3,507 metres). This finding contradicts the findings given by [16] and [34]. The hydrocarbon reservoirs are mostly found in the Agbada formation, which is located at depths ranging from around 1,000 to 4,000 metres. This distribution aligns with the geological features seen in the region. The reservoirs demonstrated a range of net pay thicknesses, varying from 23.5 feet (7.16 metres) to 739 feet (225.35 metres), highlighting their considerable economic importance.

In order to serve as reservoirs, rocks must exhibit both porosity and permeability, indicating the existence of void spaces or interconnected pathways between individual rock particles or grains [35]. The presence of these linked pores facilitates the establishment of an uninterrupted conduit for the movement of fluids. The distribution of water and hydrocarbons (oil and gas) inside the reservoirs exhibits a range of saturation levels. These levels vary from 8.1% water saturation and 91.9% to 92.1% hydrocarbon saturation, to 92.1% water saturation and 7.9% hydrocarbon saturation.

When a rock contains oil and/or gas, its resistivity exhibits an increase in comparison to the same rock when it is completely saturated with formation water [36]. Moreover, it is important to note that there is a clear correlation between the saturation of connate water and the resistivity of the formation. Specifically,

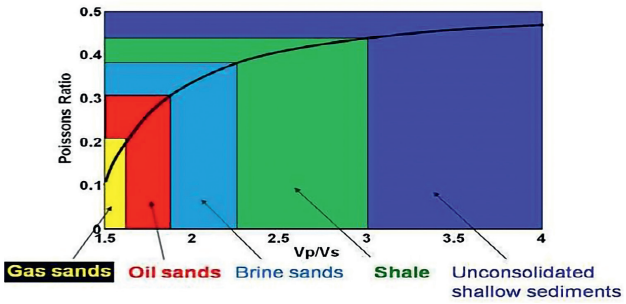

Fig. 7. Guideline for pore fluid prediction using Poisson's ratio and velocity ratio

Ryc. 7. Wskazówki pozwalające na przewidywanie ilości płynu w porach przy użyciu współczynnika Poissona i współczynnika prędkości

an increase in water saturation leads to a decrease in formation resistivity [16]. The aforementioned association establishes the significance of the formation resistivity component as a valuable indication in the identification of hydrocarbon zones. The findings of our cross-plot analysis, in conjunction with the application of a conventional cross-plot technique for estimating pore fluid using Poisson's ratio and velocity ratio, as illustrated in Figure 7, indicate that all reservoirs in the examined region can be classified into gas sand, oil sand, and brine sand categories.

The substitution of rock pores with oil and gas results in an elevation of rock resistivity. This phenomenon occurs due to the replacement of the conducting medium, water, with a non-conductive media, specifically oil and gas. The resistivity of a rock increases in tandem with the increase in the quantity of oil or gas contained within it [37]. Nevertheless, due to the inherent hydrophilic nature of rocks, a persistent water coating forms on the surface of rocks, even in the presence of significant quantities of oil and gas. This water coating serves as a conductive channel. The injection of oil or gas into the rock results in an increased resistance compared to its state when saturated with water.

In the context of the sedimentary rock sequence, it is seen that a limited subset of rock minerals demonstrates the property of electrical conductivity. Shale exhibits a decreased level of resistivity, yet the conducting agents responsible for this behaviour do not originate from the minerals present within the shale matrix [38]. In contrast, it is the ions that are affixed to the clay platelets that enable the process of electrical conduction. In contrast, oil and gas exhibit a near absence of electrical conductivity. In a rock characterised by water-filled pores, it is anticipated that the course of the current flowing through the rock, and hence its resistivity, will exhibit a correlation with the rock's porosity [39].

The lithology of the reservoirs was ascertained by the utilisation of both the Gamma log and the V_p/V_s ratio. Based on the V_p/V_s ratio values determined, Table 5 reveals that the bulk of the reservoirs can be categorised as sand-shale reservoirs.

Significant disparities can be observed in the characteristics of the cap rocks and reservoir sand units throughout the field. The cap rock, which consists of shale, demonstrates an increased Poisson ratio, as well as elastic, bulk, and stiffness moduli. Despite having lower bulk compressibility and rock strength, shale exhibits higher ductility, stiffness, reduced compressibility, and a tendency towards compressive shear failure. Additionally, it functions as a more efficient barrier for fracture stimulation.

On the other hand, the main reservoir rocks, specifically sandstones, have comparatively reduced values for the Poisson ratio, as well as the elastic, bulk, and stiffness moduli. However, these materials demonstrate increased compressibility and rock strength, making them more susceptible to brittleness and tensile failure. As a result, it has been observed that sandstones have a tendency to fracture before to shales under similar fracture gradients during hydraulic fracture stimulation [24]. Conversely, shales exhibit properties that inhibit the propagation of fractures, thereby serving as barriers. The presence of low rock strength is a contributing factor to the occurrence of wellbore failures in shale formations and weak shaly sandstones.

The elastic properties observed in the reservoirs, primarily located in the sandstone lithology, exhibit a wide range of values. Acoustic Impedance ranges from 16039.61 to 28156.01 psi, Bulk Modulus ranges

Table 5. Velocity ratio for different rock types [7]

Tabela 5. Współczynnik prędkości dla różnych typów skał [7]

Range of V_p/V_s	Rock type
0.1–1.2	Fine grained sand
1.2–1.45	Medium grained sand
1.46–1.6	Coarse grained sand
1.6–1.8	Sandstone
Above 2.0	Shale or Clay

from 7.102 to 17.634 Kbar, Shear Impedance ranges from 5929.511 to 16772.83 psi, Shear Modulus ranges from 0.729 to 9.789 Kbar, Velocity ratio ranges from 1.695 to 2.923, and Young Modulus ranges from 2.091 to 27.645 psi.

The modulus of rigidity, bulk modulus, and matrix modulus display a diminishing pattern, while the elastic moduli of the rocks exhibit an increasing tendency with increasing depth. Shale source layers, especially under anoxic conditions, contributed to the increased accumulation of hydrocarbons through the diagenetic compaction equilibrium [24]. The occurrence of shale streaks along fault lines and the development of sand caps on the tops of sand formations proved to be efficient methods for trapping substances. The compaction equilibrium is upheld by the correlation between rock compressibility, effective vertical stress, and porosity. An increase in compressibility correlates with higher levels of effective vertical stress and porosity, while a decrease in compressibility is observed with increasing depth and effective porosity. An increase in stress caused by the accumulation of silt and the expulsion of fluids initiates grain sliding and compactional deformation. As the depth increases, there is an observed drop in bulk and grain compressibility, along with a corresponding fall in pore volume [34]. The occurrence of grain-to-grain contact leads to the breakage of cement connections and causes the compaction of individual grains through elastic distortions and strains. The occurrence of impermeable sediments, such as shales, that are saturated with a fluid that cannot be compressed results in the development of overpressure as a consequence of their inherent lack of elasticity.

Abnormal pore pressures, which are a consequence of disequilibrium compaction, have been documented in various sectors of the Niger Delta [40]. The primary cause of deformation in young tertiary sedimentary rocks is compaction, which results in a gradual reduction in porosity as the rocks are buried deeper.

7. CONCLUSION

The comprehensive well log analyses conducted for Wells B001, B002, and B003 have provided valuable insights into the hydrocarbon-bearing potential of these geological formations. The data from these analyses have shed light on the characteristics of three distinct reservoirs in Well B001, two reservoirs and a water-bearing zone in Well B002, and three separate reservoirs in Well B003. These findings underscore the importance of reservoir characterization and cap rock boundaries in the evaluation of hydrocarbon prospects.

The study's findings have not only contributed to the understanding of the geological formations in the Niger Delta region but have also provided actionable insights for exploration and production endeavours. The presence of hydrocarbon reservoirs within specific depth ranges and the characterization of their attributes, including porosity, fluid saturation, and lithology, are essential considerations for decision-making in the oil and gas industry. The establishment of lithological correlations across the studied fields adds to the robustness of these insights, aiding in predicting and optimizing reservoir behaviour.

The results of this comprehensive well log analysis have implications beyond the immediate context of these specific wells. The patterns observed in porosity-depth relationships, lithological classifications, and elastic properties can potentially inform exploration strategies in similar geological formations globally. The understanding of how various factors, such as lithology, pressure, and fluid content, interplay to shape reservoir characteristics, contributes to a broader understanding of subsurface dynamics and hydrocarbon reservoir behaviour.

The thorough well log analyses conducted in Wells B001, B002, and B003 have illuminated the distinct characteristics of multiple reservoirs within the Niger Delta region. The data obtained through these analyses have revealed trends in porosity, lithology, fluid saturation, and elastic properties, offering valuable insights for making informed decisions in hydrocarbon exploration and production. By highlighting the significance of reservoir characterization and cap rock boundaries, this study serves as a foundation for further research and operational strategies in the field of geology, petrophysics, and oil and gas exploration.

- Reservoir characterization has been facilitated by a multitude of petrophysical and elastic measurements, revealing a wealth of information about the geological formations.
- The porosity determinations employing sonic, neutron, and density logs have established a consistent trend of decreasing porosity with increasing depth, in alignment with established studies. This trend is attributed to factors such as lithology, pressure, and the presence of hydrocarbons, all of

which impact porosity preservation. Furthermore, the identification of hydrocarbon-bearing zones has been supported by the relationship between formation resistivity and fluid saturation, with hydrocarbon-filled rocks exhibiting higher resistivity due to the non-conductive nature of oil and gas compared to water.

- The lithological classification based on gamma logs and the V_p/V_s ratio has facilitated a deeper understanding of the reservoirs' composition, predominantly categorizing them as sand-shale reservoirs within the Agbada Formation. This alternating arrangement of sandstones and shales is a crucial factor in the reservoir's properties and behaviour. The elastic properties exhibited within the reservoirs, particularly sandstones, have revealed important trends with depth, influencing their brittleness, strength, and susceptibility to failure under different conditions.
- The diagenetic compaction equilibrium observed in normally pressured shale source beds has played a significant role in hydrocarbon accumulation, with shale smears and sand caps serving as effective traps.

REFERENCES

1. Nwokoma, E.; Agbasi, O.E., Dinneya, O. Prediction of Litho-Porosity Using Incompressibility and Rigidity, Offshore Niger Delta, Nigeria. Geoinformatica Polonica, 2022, pp. 31–42.
2. Heap, M.J.; Kennedy, B.M. Exploring the scale-dependent permeability of fractured andesite. Earth and Planetary Science Letters, 447, 2016, pp. 139–150.
3. Nara, Y.; Meredith, P.G.; Yoneda, T. Influence of macro-fractures and micro-fractures on permeability and elastic wave velocities in basalt at elevated pressure. Tectonophysics, 503, 2011, pp. 52–59.
4. Harry, T. A.; Etim, C. E.; Agbasi O.E. Petrophysical Evaluation of H-field, Niger Delta Basin for Petroleum Plays and Prospects. Materials and Geoenvironment, 69, 2022, pp. 119–129
5. Kuffour, O. (2008). Estimation of petrophysical data for assessing hydrocarbon potential in western Ghana oil field (Tano Basin). MSc. Geophysics Report, Kwame Nkrumah University of Science and Technology.
6. Hyne, N. Nontechnical Guide to Petroleum Geology, Exploration, Drilling, and Production. Tulsa: PennWell Corporation, 2012.
7. Castagna, J.P.; Batzle, M.L.; Eastwood, R.L. Relationships between compressional and shear-wave velocities in classic silicate rocks. Geophysics. 50(4), 1985, pp. 571–581.
8. Pickett, G.R. Pattern recognitionasa meansof formation evaluation, paper A, in 14th Annual Logging Symposium Transactions: Society of Professional Well Log Analysts, 1973, pp. A1–A21.
9. Nations, J.F. Lithology and porosity from acoustic shear and compressional wave transit time relationships: Society of Petrophysicists Well Log Analysts 15th Annual Symposium 1974.
10. Miller, S.L.M.; Stewart, R.R. Effects of lithology, porosity and shaliness on P- and S-wave velocities from sonic logs: Canadian Journal of Exploration Geophysics 26, 1990, pp. 94–103.
11. Kithas, B.A. Lithology, gas detection, and rock properties from acoustic logging systems: Society of Petrophysicists Well Log Analysts 15th Annual Symposium 1976.
12. Dresser Atlas. Well logging and interpretation techniques. The course for home study, Dresser Atlas Publication, 1982.
13. Agbasi, O.E.; Esomchi, N.U.; Daniel, A.E.; Udoka, U.J. Exploring Reservoir Potential of the "X Field" Offshore, Niger Delta Basin: An Emphasis on Lithofacies, Depositional Environments, and Petrophysical Characteristics. Jurnal Penelitian Fisika Dan Aplikasinya (JPFA), 13(1), 2023, pp. 38–50.
14. Jong, S.L. Reservoir Properties Determination Using Fuzzy Logic and Neural Networks from Well Data in Offshore Korea, Journal of Petroleum Science and Engineering, 49, 2005, pp. 182–192.
15. Andisheh, A.A.; Reijers T.J.A; Nwajide C.S. Sequence stratigraphic framework of the Niger Delta. Paper presented at the AAPG international conference and exhibition, Vienna, Austria, 1997.
16. Aigbedion, I. Reservoir Fluid Differentiation case study from the Oredo Field. International, Journal of Physical Sciences, 2(6), 2007, pp. 144–148.
17. Evamy, B.D.; Haremboure, J.; Kamerling, P.; Knaap, W.A.; Molloy, F.A.; Rowlands, P.H. Hydrocarbon habitat of Tertiary Niger Delta. American Association of Petroleum Geologists Bulletin, 62, 1978, pp. 2z77–298.
18. Short, K.C.; Stäuble, A.J. Outline of geology of Niger Delta. American Association of Petroleum Geologists Bulletin, 91, 1967, pp. 761–779.
19. Inyang, N.J.; Agbasi, O.E.; Etuk, S.E.; Akaolisa, C.C.Z; Robert, U.W. Shale gas potential of Eocene shale of Agbada Formation: a paradigm shift in gas resource perception – a case study of the Niger Delta. Arabian Journal of Geosciences, 15(12), 2022, pp. 1141.
20. Okoli, A.E.; Agbasi, O.E.; Onyekuru, S.O.; Etuk, S. E. Cross plot Analysis of Rock Properties from Well Log Data for gas detection in Soku Field, Coastal Swamp Depobelt, Niger Delta Basin. Journal of Geoscience, Engineering, Environment, and Technology, 3(4), 2018, pp. 180–186.
21. Essien, U.E.; Akankpo, A.O.; Agbasi, O.E. Evaluation of reservoir's petrophysical parameters, Niger Delta, Nigeria. International Journal of Advanced Geosciences, 5(1), 2017, pp. 19–25.

22. Alao, P.A.; Ata, A.I.; Nwoke, C.E. Subsurface and Petrophysical Studies of Shaly-Sand Reservoir Targets in Apete Field, Niger Delta. International Scholarly Research Notices, ISRN Geophysics, 2013, pp. 1–11.
23. Asquith, G.; Krygowski, D. Basic Relationships of Well Log Interpretation. Basic Well Log Analysis: American Association of Petroleum Geologists Methods in Exploration 16, 2004, pp. 1–20.
24. Akpabio I.O.; Ojo, T.O. Characterization of hydrocarbon reservoir by pore fluid and lithology using elastic parameters in an x field, Niger delta, Nigeria. International Journal of Advanced Geosciences, 6(2), 2018, pp. 173––176.
25. Schlumberger, J. Log Interpretation Principles and Schlumberger Educational Services, Houston, Texas, 1987.
26. Akpabio, I.O.; Ibuot, J.C.; Agbasi O.E.; Ojo, O.T. Petrophysical Characterization of eight wells from Wire-line Logs, Niger Delta Nigeria. Asian Journal of Applied Science. 2(2), 2014, pp. 105–109.
27. Akinyokun, O.C.; Enikanselu, P.A.; Adeyemo, A.B. Adesida, A. Well log interpretation model for the determination of lithology and fluid content contents. The Pacific Journal of Science and Technology 10, 2009, pp. 507–517.
28. Imoukhai, U.C.; Mosto, O.K. Geological and Seismic Delineation of D2000 and D4000 Petroleum Reservoirs Within Afenmai Field, Niger Delta Basin, Nigeria. Earth Sciences, 11(3), 2022, pp. 69.
29. Telford, W.M.; Geldart, L.P.; Sheriff, R.E. Applied Geophysics 2nd edition (Cambridge University Press), 1976.
30. Nwokoma, E.; Agbasi, O. E.;Dinneya, O. C. Prediction of Litho-Porosity Using Incompressibility and Rigidity, Offshore Niger Delta, Nigeria. Geoinformatica Polonica, 21, 2022, pp. 31–42.
31. Friedman G.H.; Sanders J.E. Principles of Sedimentology, John Wiley & sons, New York, 1978.
32. Blatt, H.; Middleton, G.; Murray, R. Origin of Sedimentary Rocks, 2nd edition, Printice Hall, Inc., New Jersey, 1980, pp. 782.
33. Selly, R.C. Introduction to Sedimentology, 2nd edition. Academic Press, London, 1982 pp. 475.
34. Agbasi, O.E.; Igboekwe, M.U.; Chukwu, G.U.; Etuk, S.E. Discrimination of pore fluid and lithology of a well in X Field, Niger Delta, Nigeria. Arabian Journal of Geosciences, 11(11), 2018, pp. 274
35. Oluwajana, O.A.; Olugbenga, A.E.; Ehinola, O.A.; Okeugo, C.G.; Adegoke, O. Modeling hydrocarbon generation potentials of Eocene source rocks in the Agbada Formation, Northern Delta Depobelt, Niger Delta Basin, Nigeria. Journal of Petroleum Exploration and Production Technology, 7(2), 2017, pp. 379–388.
36. Obiadi, I.I.; Obiadi, C.M. Structural Deformation and Depositional Processes: Insights from the Greater Ughelli Depobelt, Niger Delta, Nigeria. Oil & Gas Research, 2, 2016, pp. 118.
37. Asubiojo, T.M.; Okunuwadje, S.E. Petrophysical Evaluation of Reservoir Sand Bodies in Kwe Field Onshore Eastern Niger Delta. Journal of Science Environment and Management, 20(2), 2016 pp. 383–393.
38. Inyang, N.; Akpabio, I.O; Agbasi, O.E. Shale volume and permeability of the Miocene unconsolidated turbidite sands of Bonga oil field, Niger delta, Nigeria. International Journal of Advanced Geosciences, 5(1), 2017, pp. 37.
39. Adeogba, A.A.; McHargue, T.R.; Graham, S.A. Transient Fan Architecture and Depositional controls from near-surface 3-D seismic data, Niger Delta Continental Slope. American Association of Petroleum Geologists Bulletin, 89(5), 2005, pp. 627–643.
40. Harry, T.A.; Etuk, S.E.; Inyang,N.; Okoli, A.E. Geomechanical evaluation of reservoirs in the coastal swamp, Niger delta region of Nigeria. International Journal of Advanced Geosciences, 6(2), 2018, pp. 165.